

Complex turbulent wakes generated by two and three side-by-side cylinders

Y. Zhou ^{*}, R.M.C. So, M.H. Liu ¹, H.J. Zhang

Department of Mechanical Engineering, The Hong Kong Polytechnic University, Hung Hom, Kowloon, Hong Kong, People's Republic of China

Received 24 March 1999; accepted 1 October 1999

Abstract

Turbulent complex wakes generated by two and three cylinders in a side-by-side arrangement were investigated experimentally. In the present context, the complex wake refers to the flow formed by two or more simple wakes behind side-by-side cylinders. One cylinder was slightly heated; the temperature difference is about 1°C so that the temperature could be treated as a passive scalar. A combination of an X-wire and a cold wire was used to measure the velocity and temperature fluctuations. The present objective is to document the turbulence field of the complex wakes and examine the interactions between turbulent simple wakes and their effects on the momentum and heat transport phenomena. It is observed that the cross-stream distributions of the Reynolds normal stresses can be asymmetrical at a small spacing-to-diameter ratio. The Reynolds shear stress and its lateral transport distributions however remain symmetrical. This is explained in terms of the gap flow deflection behind side-by-side cylinders and the transport characteristics of vortical structures. The interactions between simple wakes do not seem to have any effect on the fine-scale turbulence, at least up to the scales in the inertial sub-range. On the other hand, the temperature spectra in the inertial sub-range have been affected; their slopes have been appreciably increased compared with the single-cylinder data. The gradient transport assumption is found to be valid for the turbulence field, but not for the temperature field. The heat flux and temperature gradient do not approach zero simultaneously near the centerlines of simple wakes, thus giving rise to a substantial variation in the heat transport. This leads to a significant drop in the turbulent Prandtl number. The superposition hypothesis, as proposed by Bradshaw and his co-workers, is also examined for the present complex wakes. © 2000 Elsevier Science Inc. All rights reserved.

1. Introduction

Bradshaw (1976) defined a complex turbulent flow as one with externally applied rates of strain or where interactions of two or more basic turbulent flows are involved. Basic flows refer to simple flows such as jets, wakes, fully developed channel flows and boundary layers. For example, Fabris and Fejer (1974) formed a complex flow consisting of 31 hexagonally arranged parallel jets. Since most flows of engineering interest are complex, interest in documenting and predicting such flows is growing. The present study is primarily concerned with complex flows formed by multiple two-dimensional simple wakes generated by circular cylinders. In particular, the complex wake created by the interactions of two and three side-by-side circular cylinders is examined.

The complex wake generated by two and more cylinders has drawn considerable attention in the past due to its importance in many engineering applications. For example, complex wakes are found behind tube bundles in heat ex-

changers, fuel and control guide rods in nuclear reactors, piers and bridge pilings, oil and gas pipelines, cooling-tower arrays, suspension bridges and high rise buildings. These complex wakes are usually formed by the interactions of a number of simple wakes generated by individual structures. Research into this kind of flows has been largely focused on the Strouhal map, the pressure, the mean and fluctuating lift and drag coefficients, measured in the immediate vicinity of the cylinders (Bearman and Wadcock, 1973; Zdravkovich, 1977), while data in the downstream region is mostly limited to qualitative descriptions.

Zdravkovich (1968) conducted a smoke visualization of the laminar wake behind three-cylinders in various triangular configurations. He observed that multiple Karman vortex streets could co-exist. However, the vortices decayed very quickly and an entirely new single vortex street was formed. Williamson (1985) visualized a laminar wake with a Reynolds number ($Re = U_\infty d/\nu$) of 100–200 behind a pair of side-by-side cylinders in the range of $T/d = 1.85$ to 4.0. Here, U_∞ is the free-stream velocity, d is the diameter of the cylinders, ν is the fluid kinematic viscosity and T is the distance between the cylinder axes. He noted that, as a result of interaction, the wakes of the two cylinders could amalgamate to form a single wake. On the other hand, quantitative data on simple wake interactions is scarce. Cheng and Moretti (1988) reported the mean velocity and turbulent intensity profiles, measured by

^{*} Corresponding author.

E-mail address: mmzyzhou@polyu.edu.hk (Y. Zhou).

¹ Present address: Department of Thermal Science and Energy Engineering, The University of Science and Technology of China, People's Republic of China.

Pitot tubes, Kiel probes and hot-wires, up to $4.5d$ downstream of a single tube row with a $T/d = 1.3$. Palmer and Keffer (1972) measured an asymmetric turbulent wake generated by two side-by-side cylinders of unequal diameter at different downstream distances from the cylinders. Their aim was to create and investigate the region of turbulent ‘energy reversal’ where the turbulent kinetic energy production turns negative. However, these studies did not focus on the interaction between the individual wakes. Fabris (1984) studied the interaction of two turbulent wakes generated by a pair of cylinders in a side-by-side arrangement. The T/d ratio was set at 8 and his measurements were carried out in the far field. From this brief review, it is evident that the near field interactions of simple wakes have not been extensively investigated. Therefore, the major objective of the present work is to assess the interactions in the near field of simple wakes generated by individual circular cylinders and attempts to provide a reliable documentation for the Reynolds stresses and heat fluxes, which is important for developing and fine-tuning turbulence models.

Investigation of heat transport in a complex wake can be achieved by slightly heating one cylinder. As such, the coupling between the velocity and the temperature field can be neglected and the temperature can be treated as a passive scalar. Another advantage of a small temperature difference between the cylinder and the ambient fluid is that the temperature sensitivity of the hot wire can be ignored when transforming the hot-wire voltages into velocities. This is beneficial to the present investigation because hot-wires are used to measure the velocity field. Furthermore, the investigation allows the turbulent Prandtl number to be examined. This data is important for the thermal eddy diffusivity model because it is used in conjunction with the eddy diffusivity for momentum to evaluate the thermal eddy diffusivity. Note that the use of turbulent heat transfer models at a level higher than the thermal eddy diffusivity model is less well developed and rather complicated (Kays, 1994; So and Speziale, 1999). However, the use of a diffusivity model requires the assumption of gradient transport. Consequently, the validity and extent of the gradient transport assumption is examined for both heat and momentum transport in the complex wakes.

Bradshaw et al. (1973) proposed a superposition scheme. According to their hypothesis, when two simple shear layers merged to form a complex shear layer, the characteristics of the complex shear layer could be deduced from the individual simple shear layer providing the interaction effects were weak on the turbulence structures. In other words, the turbulence fields of the two simple shear layers could be superimposed to form the turbulence field of the complex shear layer. It is well known that the non-linear Navier–Stokes equations forbid the superposition of two or more turbulence fields. However, this hypothesis seemed to be quite valid for those flows that were formed by interactions of shear layers. They demonstrated that, based on the hypothesis, a fully developed duct flow could be well predicted by a calculation method using empirical data obtained from isolated fully developed boundary layers. Weir et al. (1981) did similar calculation for a plane jet using the data of two mixing layers that originated at the two lips of the jet nozzle. They found that there was fairly good agreement between calculations and measurements, except for the triple velocity products near the centerline. The validity of the superposition hypothesis was further substantiated by the calculation of a turbulent near-wake of a flat plate using the data of the two shear layers developed on opposite sides of the plate (Andreopoulos and Bradshaw, 1980). These studies seem to suggest that the non-linear effects of interactions between the shear layers might be quite small, possibly up to the second order of velocity products. In the present investigation,

the hypothesis for the complex wakes formed by the interactions of two or more simple wakes will be further examined. Since the hypothesis has not been tested against this type of flows before, it is of interest to assess the extent to which the hypothesis is valid. Furthermore, the extent to which the hypothesis is invalid can reflect the non-linear effects of interactions between the simple wakes.

2. Experimental details

Experiments to investigate the behavior of complex wakes were carried out in an open-return, low turbulence wind tunnel with a square cross-section ($0.3 \text{ m} \times 0.3 \text{ m}$) of 0.8 m long. The wakes were generated by one, two or three brass cylinders ($d = 3.8 \text{ mm}$) arranged side-by-side (Fig. 1). The cylinders were installed horizontally in the mid-plane and spanned the full width of the working section. They were located at 20 cm downstream of the exit plane of the contraction. This resulted in a maximum blockage of about 3.8% and an aspect ratio of 79. The transverse spacing between the cylinders was varied from $T/d = 1.5$ to 3. Only cylinder 1 (Fig. 1) was electrically heated in these experiments. The maximum temperature difference between the cylinder and the ambient fluid, Θ_1 , was approximately 0.8 – 1.1°C . At this level of heating, the temperature can be safely treated as a passive scalar at the two measurement stations, $x/d = 10$ and 20 , where x is the stream-wise coordinate measured from the center of the cylinder. Measurements were made at a free-stream velocity U_∞ of 7 m/s , or $Re = 1800$. In the free-stream, the longitudinal turbulence intensity was measured to be approximately 0.5% .

A three-wire probe (an X-wire plus a cold wire, the latter placed about 1 mm upstream of the X-wire crossing point and orthogonal to the X-wire plane) was used to measure the velocity fluctuations in the stream-wise and lateral directions, u and v , respectively, and the temperature fluctuation, θ . The hot wires were etched from a $5 \mu\text{m}$ diameter Wollaston (Pt–10% Rh) wire to a length of about 1 mm . As for the cold wire, a $1.27 \mu\text{m}$ diameter Wollaston (Pt–10% Rh) wire was etched to a length of about 1.2 mm and a temperature coefficient of $1.69 \times 10^{-3} \text{ }^\circ\text{C}^{-1}$ (Browne and Antonia, 1986) was used. Constant-temperature and constant-current circuits were used for the operation of the hot wires and the cold wire, respectively. An overheat ratio of 1.8 was adopted for the X-wire, while a current of 0.1 mA was used in the cold wire. The sensitivity of the cold wire to velocity fluctuations was negligible since the length-to-diameter ratio was about 1000, sufficiently large to allow the neglect of any low-wave-number attenuation of the temperature variance. Based on Antonia et al. (1981) the fre-

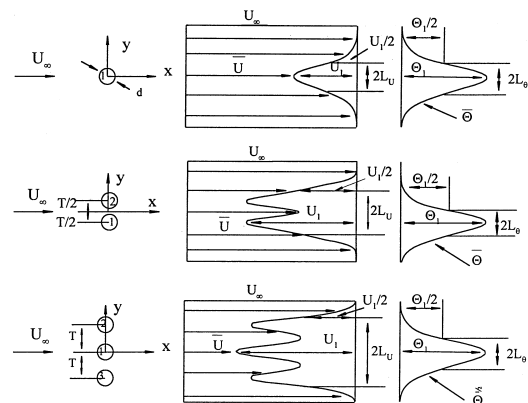


Fig. 1. Definition sketch.

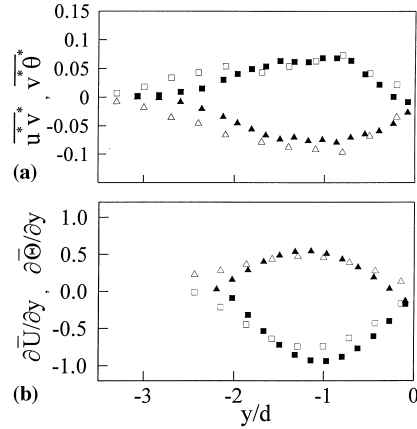


Fig. 2. Comparison between the present measurement ($Re = 5900$, solid symbols) and Antonia et al. (1993) data ($Re = 5830$, open symbols): (a) \overline{uv}/U_1^2 (■, □); $v\theta/U_1\theta_1$ (▲, △); (b) $\partial\overline{U}/\partial y$ (■, □: extracted from Antonia et al.'s data), $\partial\overline{\theta}/\partial y$ (▲, △: extracted from Antonia et al., data) $x/d = 10$.

quency response of the wire, as indicated by -3 dB frequency, was estimated to be 2.2 kHz at the wind speed investigated. This was sufficient to avoid any high frequency attenuation of the main quantities of interest to the present study. Signals from the circuits were offset, amplified and then digitized using a 16 channel (12 bit) A/D board and a personal computer at a sampling frequency of 3.5 kHz per channel. The duration of each record was about 15 s.

In order to compare with published data, a cylinder with $d = 12.7$ mm was also used in the single cylinder configuration. Other experimental conditions were unchanged, including U_∞ , which was maintained at 7 m/s. The resulting Re was about 5900. Fig. 2 presents a comparison between the present measurements and those of Antonia et al. (1993). The asterisk is used in the figure to denote normalization by the maximum mean velocity and mean temperature deficit, U_1 and θ_1 , of the corresponding wake. They show good agreement in the Reynolds shear stress \overline{uv} , the heat flux $v\theta$, and the gradients $\partial\overline{U}/\partial y$ and $\partial\overline{\theta}/\partial y$ of the mean velocity \overline{U} and the mean temperature $\overline{\theta}$, thus providing a validation of the present measurements.

3. Turbulent statistics

In this study, the single-cylinder wake is a simple wake and can be used as a benchmark to investigate the effects of interactions between simple wakes that were generated by the side-by-side cylinders. Therefore, the data of the single-cylinder wake is also presented (Fig. 3) for comparison and for use in the superposition hypothesis calculations. In the following, the turbulent statistics of the complex wakes are discussed and their similarity to the simple wake will be pointed out.

Mean velocity. Figs. 4 and 5 present the cross-stream distribution of the mean velocity in the two- and three-cylinder wakes. As T/d reduces, the multiple peaks in Figs. 4(a),(c) and 5(a),(c) merge into one (Figs. 4(b) and (d), 5(b) and (d)), thus showing the tendency to form a single wake, much like that of the single cylinder wake shown in Fig. 3.

Second-order products. Measured shear stress \overline{uv} and normal stresses $\overline{u^2}$ and $\overline{v^2}$ are presented in Figs 6–11. The cross-stream distributions of $\overline{u^2}$ and $\overline{v^2}$ exhibit asymmetry at $T/d = 1.5$ (Figs. 6–9) and, as suggested in Figs. 7(b) and (d),

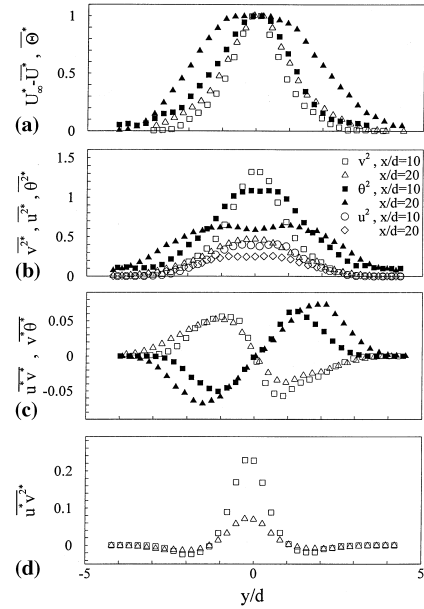


Fig. 3. Lateral distributions of (a) mean velocity (open symbols) and temperature (solid symbols); (b) streamwise and transverse velocity (open symbols) and temperature variance (solid symbols); (c) shear stress (open symbols) and heat flux (solid symbols) in a single cylinder wake. (■, □) $x/d = 10$; (▲, △) $x/d = 20$.

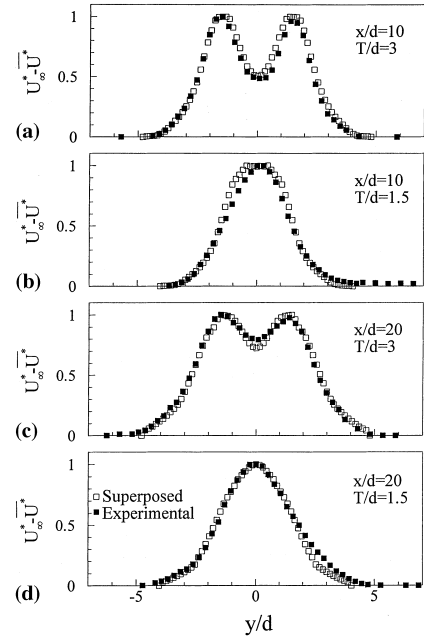


Fig. 4. Measured mean streamwise velocity (■) and calculation (□) based on superposition hypothesis in a two-cylinder wake.

could be oppositely skewed for different measurements. It has been reported by Ishigai et al. (1972) that, when T/d is between 1.5 and 2.0, the gap flow between the individual simple wakes could stably deflect and the vortex streets could become asymmetric with respect to $y = 0$. This phenomenon would become much worse when $T/d < 1.5$ (Williamson, 1985; Moretti, 1993). Zhou and Antonia (1994) studied a turbulent near-wake in terms of critical points. They referred to the

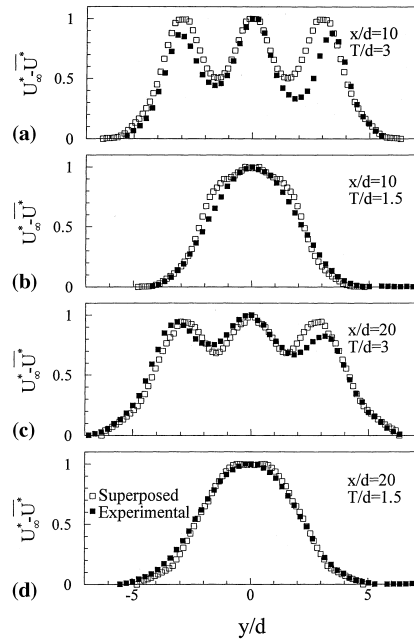


Fig. 5. Measured mean streamwise velocity (■) and calculation (□) based on superposition hypothesis in a three-cylinder wake.

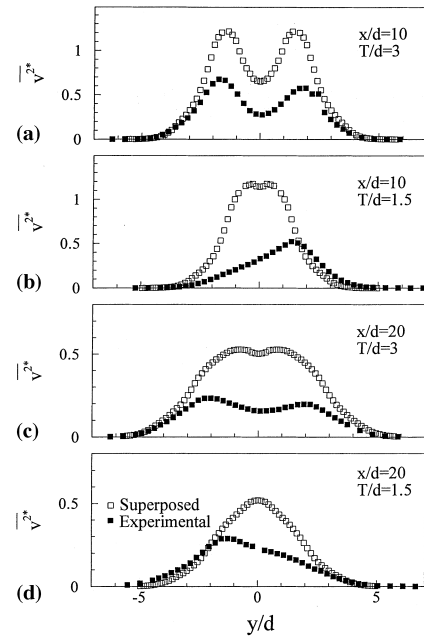


Fig. 7. Measured $\overline{v^2}$ (■) and calculation (□) based on superposition hypothesis in a two-cylinder wake.

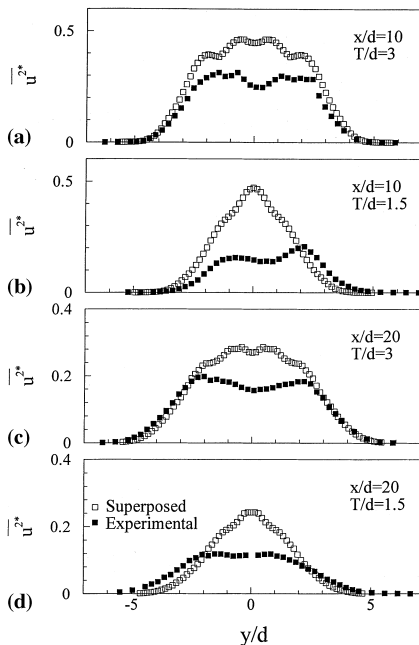


Fig. 6. Measured $\overline{u^2}$ (■) and calculation (□) based on superposition hypothesis in a two-cylinder wake.

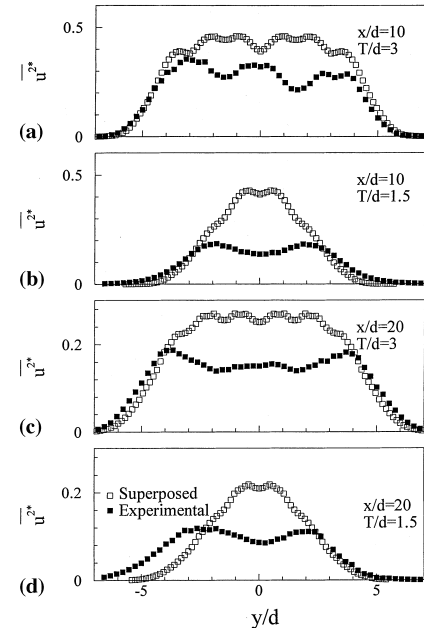


Fig. 8. Measured $\overline{u^2}$ (■) and calculation (□) based on superposition hypothesis in a three-cylinder wake.

region around the vortex centres as the focal region and the region around saddle points between two consecutive vortices as the saddle region. The focal region actually represents the large-scale vortical structure or the vortex. They observed that the focal region contributed most to $\overline{u^2}$ and $\overline{v^2}$. Consequently, the asymmetry of the vortex streets could lead to the asymmetric distributions of the measured $\overline{u^2}$ and $\overline{v^2}$. On the other hand, \overline{uv} (Figs. 10 and 11) is anti-symmetrical with respect to $y = 0$. Due to the cancellation of positive and negative uv products associated with the vortices, the contribution to \overline{uv} is

not from the focal region but mostly from the saddle region (Zhou and Antonia, 1993, 1994). Therefore, the asymmetry of vortex streets may not significantly affect the \overline{uv} distribution.

Since heat is associated with vortical structures, the heat flux $\overline{v\theta}$ (Fig. 12) is affected by the deflected vortex streets, exhibiting asymmetry at $T/d = 1.5$. At $T/d = 3.0$, $\overline{v\theta}$ (Fig. 12(c)) is anti-symmetric with respect to the centreline of the heated simple wake in the three-cylinder case. The anti-symmetry deviates appreciably in the two-cylinder wake (Figs. 12(a)). Evidently, the interaction is symmetrical around the centreline of the heated simple wake in the three-cylinder case but not in

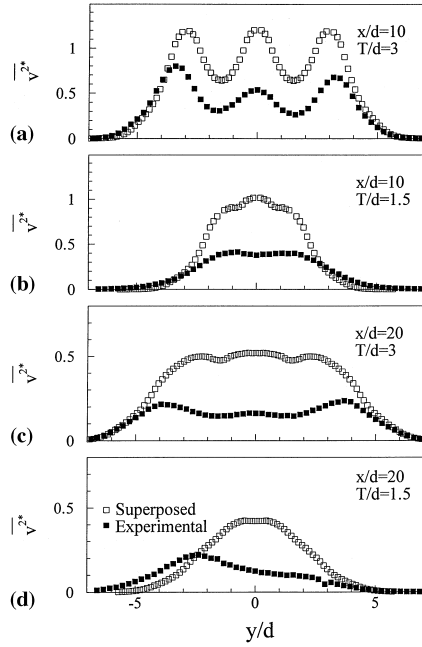


Fig. 9. Measured $\overline{v^2}$ (■) and calculation (□) based on superposition hypothesis in a three-cylinder wake.

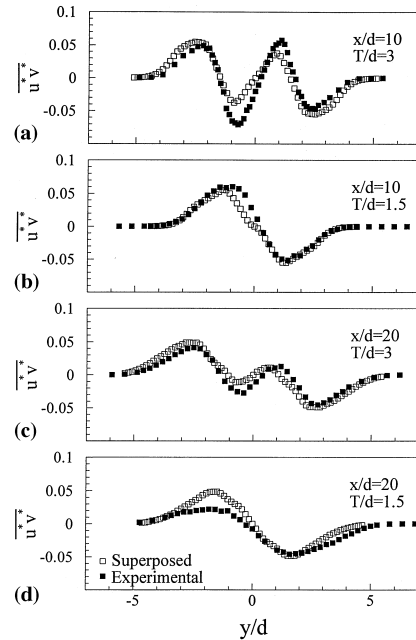


Fig. 10. Measured \overline{uv} (■) and calculation (□) based on superposition hypothesis in a two-cylinder wake.

the two-cylinder case. This demonstrates that the interaction between simple wakes, though relatively weak, is not negligible.

Third-order velocity products. Figs. 13 and 14 present the results of the lateral transport of the shear stress, $\overline{uv^2}$, for the two- and three-cylinder wakes. The $\overline{uv^2}$ distribution is quite symmetrical with respect to $y = 0$. For the same reason as that explained in the behavior of \overline{uv} , most of the contribution to $\overline{uv^2}$ is not from the focal region; instead, it is most likely derived

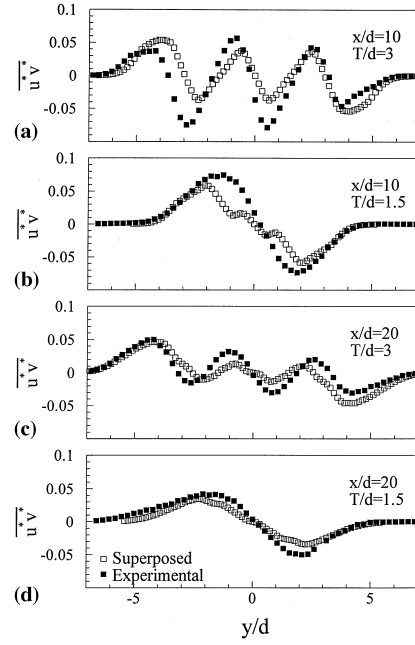


Fig. 11. Measured \overline{uv} (■) and calculation (□) based on superposition hypothesis in a three-cylinder wake.

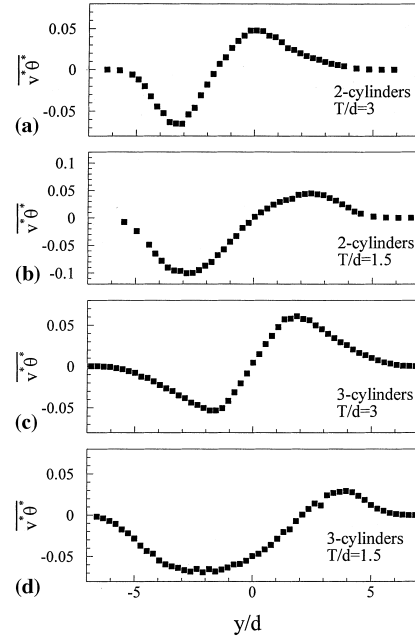


Fig. 12. Measured $\overline{v\theta}$ in two-cylinder (a, b) and three-cylinder wakes (c, d). $x/d = 20$.

from the saddle region. Therefore, $\overline{uv^2}$ is insensitive to the asymmetry of the vortex streets.

4. Gradient transport assumption

The single- and three-cylinder wake data are reasonably symmetrical about the centreline ($y/d = 0$) of the heated cylinder. In the case of the two-cylinder wake, only the lower

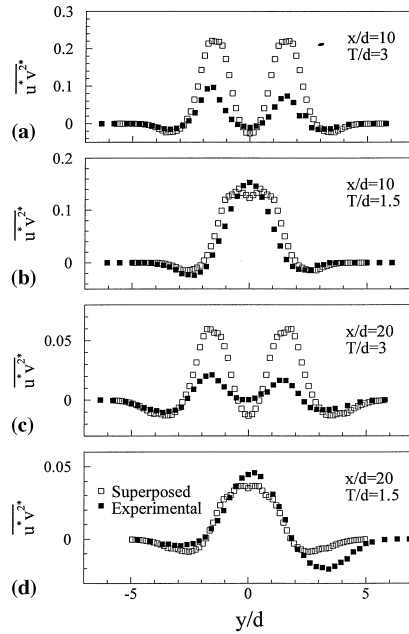


Fig. 13. Measured $\overline{uv^2}$ (■) and calculation (□) based on superposition hypothesis in a two-cylinder wake.

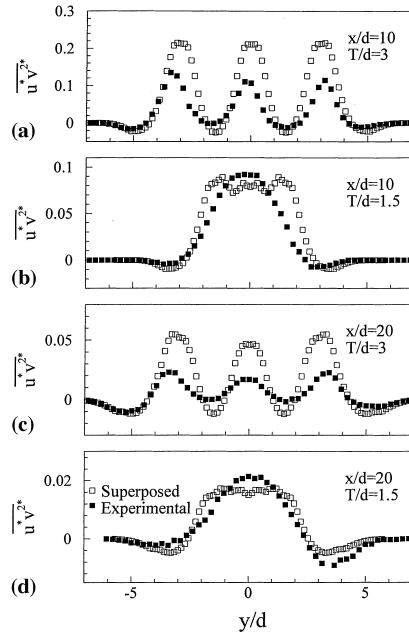


Fig. 14. Measured $\overline{uv^2}$ (■) and calculation (□) based on superposition hypothesis in a three-cylinder wake.

cylinder was heated. This arrangement allows the interactions between two asymmetric turbulent simple wakes, one heated and the other not, to be investigated. The asymmetric nature of this arrangement is quite different from that of the single-cylinder and the three-cylinder case. The spread of the thermal boundary was comparable with that of the turbulent flow on the lower side ($y/d < 0$), but was entirely contained within a fully turbulent fluid on the upper side ($y/d > 0$).

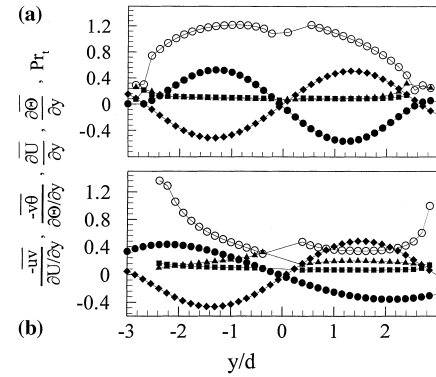


Fig. 15. Lateral distributions of $-\overline{u\theta}/(\partial\overline{U}/\partial y)$ (■), $-\overline{v\theta}/(\partial\overline{\theta}/\partial y)$ (▲), $\partial\overline{U}/\partial y$ (◆), $\partial\overline{\theta}/\partial y$ (●), and the turbulent Prandtl number (○) in a single cylinder wake: (a) $x/d = 10$; (b) $x/d = 20$.

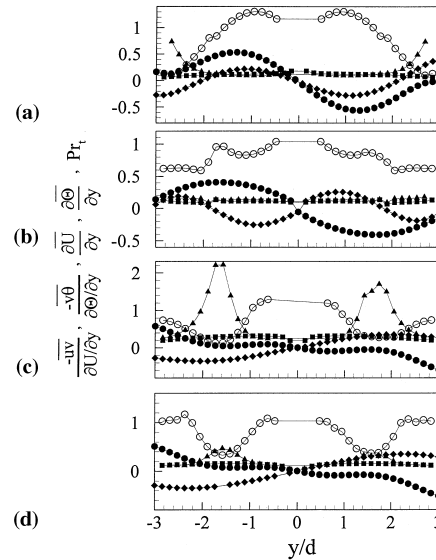


Fig. 16. Lateral distributions of $-\overline{u\theta}/(\partial\overline{U}/\partial y)$ (■), $-\overline{v\theta}/(\partial\overline{\theta}/\partial y)$ (▲), $\partial\overline{U}/\partial y$ (◆), $\partial\overline{\theta}/\partial y$ (●), and the turbulent Prandtl number (○) in a three-cylinder wake: (a) $x/d = 10$, $T/d = 3.0$; (b) 20 , 3.0 ; (c) 10 , 1.5 ; (d) 20 , 1.5 .

Figs. 15 and 16 present the transverse distributions of the gradients, $\partial\overline{U}/\partial y$ and $\partial\overline{\theta}/\partial y$, and the ratios, $-\overline{u\theta}/(\partial\overline{U}/\partial y)$ and $-\overline{v\theta}/(\partial\overline{\theta}/\partial y)$. The gradients were estimated from a least-squares (seventh-order polynomial) fit to \overline{U} and $\overline{\theta}$. In the single-cylinder wake, the gradient transport assumption is quite valid, that is, the shear stress approaches zero at the same location as the mean velocity gradient. The heat flux and the temperature gradient also become zero simultaneously (Fig. 2). The ratio $-\overline{u\theta}/(\partial\overline{U}/\partial y)$ is virtually a constant, so is $-\overline{v\theta}/(\partial\overline{\theta}/\partial y)$. In the complex wakes, because of weak interactions, the gradient transport assumption is only valid at $T/d = 3.0$. When the separation distance is reduced to $T/d = 1.5$, the gradient transport assumption is still valid for the momentum transport. However, $\overline{v\theta}$ (Fig. 12) does not necessarily approach zero near the centrelines of the individual simple wakes when $\partial\overline{\theta}/\partial y$ goes to zero (Figs. 16(c) and (d)). Consequently, $-\overline{v\theta}/(\partial\overline{\theta}/\partial y)$, which otherwise is approximately constant, changes significantly at $y/d = 0$ and ± 1.5 .

5. Turbulent Prandtl number

The turbulent Prandtl number, Pr_t , defined as

$$Pr_t = \frac{\overline{uv}/(\partial\overline{U}/\partial y)}{\overline{v\theta}/(\partial\overline{\theta}/\partial y)} = \frac{\overline{uv}}{\overline{v\theta}} \frac{\partial\overline{\theta}}{\partial\overline{U}}$$

is also shown in Figs. 15 and 16. In these figures, Pr_t was estimated from the values of \overline{uv} , $\overline{v\theta}$, and a least-squares (seventh-order polynomial) fit to the mean temperature $\overline{\theta}$ versus the mean velocity \overline{U} . This method of determining Pr_t is similar to that used by Pimenta et al. (1979). The resulting uncertainty in Pr_t was estimated from the uncertainties in, and $\partial\overline{\theta}/\partial\overline{U}$ and was found to be about 17% (Antonia et al., 1993). Note that the centreline of the wakes is a singular point of Pr_t . Therefore, data near the centreline have been removed.

The Pr_t values measured at $x/d=10$ for the single-cylinder wake are approximately equal to 1 when $y/d<2$, thus indicating that the Reynolds analogy is quite valid; it drops substantially at $x/d=20$ though. This agrees well with the findings of Antonia et al. (1993). However, no explanation was attempted in their report. Fig. 15(b) indicates that $\partial\overline{\theta}/\partial y$ experiences a faster decrease in magnitude than $\partial\overline{U}/\partial y$ in the region, $x/d=10$ to 20, probably because the mixing of a passive scalar is accelerated substantially by the interactions between simple wakes. Subsequently, $-\overline{v\theta}/(\partial\overline{\theta}/\partial y)$ is increased in magnitude, resulting in a significant drop in Pr_t .

In the near field ($x/d\sim 20$) of complex wakes, as shown in Fig. 16(c) and (d), Pr_t decreases substantially near the centrelines of individual simple wakes since the heat transport $-\overline{v\theta}/(\partial\overline{\theta}/\partial y)$ increases in magnitude in these locations. Otherwise, Pr_t should be approximately unity.

6. Spectral characteristics

Examination of spectra may indicate the extent to which the turbulent structures have been affected by the interaction between simple wakes. Fig. 17 presents some typical spectra E_u , E_v and E_θ of u , v and θ at $x/d=20$ and $0.5d$ above the centreline of the heated simple wake generated by cylinder 1 (Fig. 1). All spectra exhibit a peak at the average vortex shedding frequency f_s . When $T/d=3.0$, the Strouhal number, $f_s d/U_\infty$, of the two- and three-cylinder wake is identical to that of the single-cylinder wake (~ 0.21). However, as T/d is reduced to 1.5, $f_s d/U_\infty$ drops to 0.104 in the two-cylinder case and to 0.065 in the three-cylinder case. It is well documented that when T/d is between 1.5 and 2.0, two vortex-shedding frequencies occur in the wake of a cylinder row. This result is confirmed by the present experiment. It is further noted that the two frequencies ($f_s d/U_\infty = 0.104$ and 0.102) in the two-cylinder wake are not the same as those (0.067 and 0.065) in the three-cylinder wake. It seems that the shedding frequencies are also dependent on the number of cylinders.

In the single-cylinder wake, the slope of the inertial sub-range of E_θ is $-5/3$ for the present Reynolds number $Re=1800$. The slope is consistent with that documented in the literature, e.g., Tennekes and Lumley (1972) and Sreenivasan (1996). The slopes of the inertial sub-range of E_u and E_v are identical to that of E_θ . The present measurement of the slope is the same as Sreenivasan's (1996) observation for E_u but slightly larger for E_v in the same Reynolds number range. In the complex wakes, the inertial sub-range of E_u and E_v does not appear to be affected by the interactions between the simple wakes. As a result, the slope remains the same as in the single-cylinder case. This, however, is not the case for E_θ . There is an appreciable increase, up to $-9/3$, in the magnitude of the slope of the inertial sub-range in all the complex wakes.

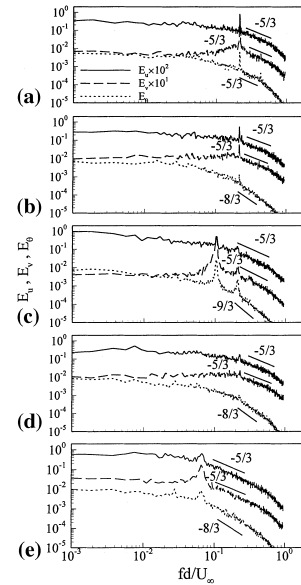


Fig. 17. Power spectra E_θ , E_u and E_v of the fluctuating temperature (θ), streamwise and lateral velocities (u , v), $x/d=20$: (a) single cylinder, $y/d=0.5$; (b) two cylinders, $T/d=3.0$, $y/d=-1.0$; (c) two cylinders, $T/d=1.5$, $y/d=-0.25$; (d) three cylinders, $T/d=3.0$, $y/d=0.5$; (e) three cylinders, $T/d=1.5$, $y/d=0.5$.

It is evident that the interactions between simple wakes affect not only large-scale temperature fluctuations but also the fine scales in the inertial sub-range.

7. Calculation based on the superposition hypothesis

As seen in Section 4, the gradient transport assumption is generally valid for the velocity field irrespective of the transverse spacing between cylinders. This suggests that the velocity fields of individual simple wakes might be superposable to represent to some extent the corresponding complex wake. From another perspective, the extent to which the hypothesis is invalid can reflect the non-linear effects of interactions between the simple wakes. The data of the single-cylinder wake (Fig. 3) was used to calculate the turbulence field of the complex wakes based on the superposition hypothesis, viz. $F = \sum_{i=1}^2 \text{ or } 3 F_i$, where F is a turbulent quantity at a spatial location of a complex wake and F_i the contribution from the i th simple wake. The calculations are compared with the measured data of the complex two- and three-cylinder wakes.

Mean velocity. The measurements and the predictions from the superposition hypothesis (Figs. 4 and 5) are in agreement with each other, irrespective of the x/d locations and the cylinder separation distance T/d . The discrepancies are within experimental uncertainty, which is about $\pm 2\%$ (Zhou and Antonia, 1992), and are mainly caused by the velocity calibration of the X-wire. It is evident from these results that the superposition hypothesis is quite valid for the two- and three-cylinder wakes, as far as the mean field of the complex wake is concerned.

Second-order velocity products. The \overline{uv} calculated according to the superposition hypothesis agree reasonably well, both qualitatively and quantitatively, with measurements (Figs. 10 and 11). However, discrepancies are noticed in $\overline{u^2}$ and $\overline{v^2}$ (Figs. 6–9). At $T/d=3.0$, the calculated $\overline{u^2}$ and $\overline{v^2}$ are in qualitative agreement with the measurements, but is substantially

smaller in magnitude. This indicates that the effect of the non-linear interference between simple wakes, though relatively weak, is appreciable in terms of second-order velocity products and perhaps higher orders. The discrepancies worsens at $x/d = 20$. This is probably because the wake growth intensifies the non-linear effects of interactions between simple wakes as x/d increases, thus giving rise to a substantial change in the turbulence structure. When T/d reduces to 1.5, the calculation based on the superposition hypothesis fails to yield results that are consistent with the experimental data, qualitatively as well as quantitatively. Since the superposition hypothesis does not take the gap flow deflection into account, it is not surprising that the calculations are in poor agreement with the measurements at $T/d = 1.5$. The significant difference in behavior in the calculations of \overline{uv} , $\overline{u^2}$ and $\overline{v^2}$ based on the superposition hypothesis seems to suggest that the shear stress and the normal stresses could develop rather differently in a complex wake.

Third-order velocity products. The calculation of $\overline{uv^2}$ (Figs. 13 and 14) based on the superposition hypothesis appears to be in reasonable agreement with experiment, except near $y/d = 0$ for the $T/d = 1.5$ case. However, the results show considerable discrepancies for the $T/d = 3.0$ case.

Based on the superposition hypothesis, Bradshaw et al. (1973) successfully predicted a fully developed plane duct flow using the data of two fully developed isolated boundary layers. They concluded that the interactions between the boundary layers did not significantly change the turbulence structure. The relatively weak effects of interactions could be attributed to the ‘time-sharing’ process of large eddies. In other words, the large eddies from either shear layer could occur at the same location but not at the same time. Weir et al. (1981) formed a two-dimensional jet by superposing two mixing layers, and found that the triple velocity products near the centreline were significantly affected by the interactions. They suggested that the relatively high turbulent intensities in the mixing layers gave rise to an intense interaction and significant non-linear effects. Andreopoulos and Bradshaw (1980) investigated the interaction between turbulent shear layers in the near-wake of a flat plate and proposed that interactions took place by fine-grain mixing, instead of large eddy ‘time sharing’. In the complex wakes investigated in this study, it is most likely that the interactions occur through opposite-sign large-scale eddies from the different simple wakes. Therefore, fine-grain mixing could not have played a dominant role. In addition, intense interactions and non-linear effects could be expected because of the relatively high turbulent intensities in the wake. The poor agreement in $\overline{u^2}$, $\overline{v^2}$ and $\overline{uv^2}$ is therefore not unexpected. Evidently, the interactions have altered the turbulence structure and cannot be completely represented by the ‘time sharing’ process of large eddies. Williamson (1985) observed that, in the range of $Re = 100$ to 200, the vortex streets behind two cylinders might be anti-phase as well as in-phase. However, the anti-phase vortex streets appeared to be dominating. The two configurations of vortex streets have also been noted at higher Re ; see for example Kamemoto (1976) at $Re = 662$. It seems plausible that the in-phase vortex streets are consistent with the time-sharing concept of large eddies. Therefore, it is likely that the strong interactions occur between the anti-phase vortex streets. Since the lateral velocities associated with the interacting vortices in two anti-phase streets have opposite signs, they tend to cancel out each other, thus leading to a smaller $\overline{v^2}$. On the other hand, the interaction between the in-phase streets may not be negligible; the streamwise velocities associated with the interacting vortices in two in-phase streets have opposite signs, the ensuing cancellation resulting in a smaller $\overline{u^2}$. This could provide an explanation as to why the

calculations based on the superposition hypothesis are substantially larger than the measurements in Figs. 6–9.

8. Conclusions

The complex wakes and the effects of interactions between simple wakes on the velocity field and the temperature field have been investigated using a three-wire probe. This investigation leads to the following conclusions.

(1) The interaction between simple wakes at $T/d = 3.0$, though relatively weak, is not negligible in terms of second- and higher-order velocity products and heat flux. As T/d reduces to 1.5, the cross-stream distribution of the heat flux $\overline{v\theta}$ and the Reynolds normal stresses $\overline{u^2}$ and $\overline{v^2}$ is skewed and the skew direction appears arbitrary. The observation is consistent with the bi-stable gap flow deflection behind side-by-side cylinders. On the other hand, the cross-stream distributions of the Reynolds shear stress \overline{uv} and its lateral transport $\overline{uv^2}$ remain anti-symmetric and symmetric, respectively; they do not seem to be affected in any significant way by the gap flow deflection. In a turbulent near-wake, the vortical structure accounts for most of the contribution to $\overline{u^2}$ and $\overline{v^2}$. As a consequence, the deflected vortex streets could give rise to the asymmetry of $\overline{u^2}$ and $\overline{v^2}$. Since heat is associated with vortical structures, the heat flux $\overline{v\theta}$ is affected by the deflected vortex streets. However, the contributions to \overline{uv} and $\overline{uv^2}$ are mostly from the saddle region and not from the vortical structure. Therefore, their distributions are insensitive to the deflection of the vortex streets.

(2) The gradient transport assumption has been validated in terms of momentum transport in both simple and complex wakes. The assumption, however, does not seem to be always valid in terms of passive scalar transport in complex wakes. It is found that $\overline{v\theta}$ and $\partial\overline{\theta}/\partial y$ do not approach zero simultaneously near the centrelines of the simple wakes that make up the complex wake. This leads to an increase in $-\overline{v\theta}/(\partial\overline{\theta}/\partial y)$ and subsequently a significant drop in the turbulent Prandtl number.

(3) In the single-cylinder wake, the turbulent Prandtl number is near unity at $x/d = 10$, but decreases substantially at $x/d = 20$ due to a faster decrease in $\partial\overline{\theta}/\partial y$ than in $\partial\overline{U}/\partial y$. The Prandtl number is affected by the interactions between simple wakes; it drops substantially near the centrelines of the simple wakes that make up the complex wake.

(4) The interactions between simple wakes do not seem to have any effect on the fine-scale turbulence of the velocity field, at least up to the inertial sub-range of the velocity spectra. However, the inertial sub-range of the temperature spectra has been affected significantly. This reflects in a substantial change in the slope of the inertial sub-range.

(5) The superposition hypothesis can be used to predict quite well the mean velocity fields and the Reynolds shear stress of complex cylinder wakes using the experimental data of a single-cylinder wake. However, significant discrepancies between measurements and calculations exist for the Reynolds normal stresses and the third-order velocity products. Evidently, the turbulence structure has been altered, which may be attributed to the gap flow deflection as well as the non-linear interactions between simple wakes.

Acknowledgements

The authors wish to acknowledge the financial support given to them by The Hong Kong Polytechnic University through Grant No. G-V396 and the Research Grants Council

of the Government of the HKSAR through Grant No. PolyU5161/97E.

References

- Andreopoulos, J., Bradshaw, P., 1980. Measurements of interacting turbulent shear layers in the near wake of a flat plate. *J. Fluid Mech.* 100, 639–668.
- Antonia, R.A., Browne, L.W.B., Chambers, A.J., 1981. Determination of time constants of cold wires. *Rev. Sci. Instr.* 52, 1382–1385.
- Antonia, R.A., Zhou, Y., Matsumura, M., 1993. Spectral characteristics of momentum and heat transfer in the turbulent wake of a circular cylinder. *Experimental Thermal Fluid Sci. J.* 6, 371–375.
- Bearman, P.W., Wadcock, A.J., 1973. The interaction between a pair of circular cylinders normal to a stream. *J. Fluid Mech.* 61, 499–511.
- Bradshaw, P., Dean, R.B., McEligot, N.P., 1973. *Trans. ASME I J. Fluids Eng.* 95, 214.
- Bradshaw, P., 1976. In: Koiter, K.T. (Ed.), *Theoretical and Applied Mechanics*, North Holland, Amsterdam, p. 101.
- Browne, L.W.B., Antonia, R.A., 1986. Reynolds shear stress and heat flux measurements in a cylinder wake. *Phys. Fluids* 29, 709–713.
- Cheng, M., Moretti, P.M., 1988. Experimental study of the flow field downstream of a single tube row. *Experimental Thermal Fluid Sci. J.* 1, 69–74.
- Fabris, G., 1984. A conditional-sampling study of the interaction of two turbulent wakes. *J. Fluid Mech.* 140, 355–372.
- Fabris, G., Fejer, A.A., 1974. Confined mixing of multiple jets. *J. Fluids Eng.* 96, 92–95.
- Ishigai, S., Nishikawa, E., Nishimura, K., Cho, K., 1972. Experimental study on structure of gas flow in tube banks with tube axes normal to flow. Part 1, Karman vortex flow around two tubes at various spacings. *Bull. JSME* 15, 949–956.
- Kamemoto, K., 1976. Formation and interaction of two parallel vortex streets. *Bull. JSME* 19, 283–290.
- Kays, W.M., 1994. Turbulent Prandtl number – where are we? *J. Heat Transfer* 116, 284–295.
- Moretti, P.M., 1993. Flow-induced vibrations in arrays of cylinders. *Annual Rev. Fluid Mech.* 25, 99–114.
- Palmer, M.D., Keffer, J.F., 1972. An experimental investigation of an asymmetrical turbulent wake. *J. Fluid Mech.* 53, 593–610.
- Pimenta, M.M., Moffat, R.J., Kays, W.M., 1979. The structure of a boundary layer on a rough wall with blowing and heat transfer. *J. Heat Transfer* 101, 193–197.
- So, R.M.C., Speziale, C.G., 1999. In: Tien, C.L. (Ed.), *A review of heat transfer modeling. Annual Review of Heat Transfer-X*, Begell House, New York, pp. 177–219.
- Sreenivasan, K.R., 1996. The passive scalar spectrum and the Obukhov–Corrsin constant. *Phys. Fluids* 8, 189–196.
- Tennekes, H., Lumley, J.L., 1972. *A First Course in Turbulence*, MIT Press, Boston, MA, p. 286.
- Weir, A.D., Wood, D.H., Bradshaw, P., 1981. Interacting turbulent shear layers in a plane jet. *J. Fluid Mech.* 107, 237–260.
- Williamson, C.H.K., 1985. Evolution of a single wake behind a pair of bluff bodies. *J. Fluid Mech.* 159, 1–18.
- Zdravkovich, M.M., 1968. Smoke observation of the wake of a group of three-cylinders at low Reynolds number. *J. Fluid Mech.* 32, 339–351.
- Zdravkovich, M.M., 1977. Review of flow interference between two circular cylinders in various arrangements. *J. Fluids Eng.* 99, 618–633.
- Zhou, Y., Antonia, R.A., 1992. Convection velocity measurements in a cylinder wake. *Exp. Fluids* 13, 63–70.
- Zhou, Y., Antonia, R.A., 1994. Critical points in a turbulent near-wake. *J. Fluid Mech.* 275, 59–81.
- Zhou, Y., Antonia, R.A., 1993. A study of turbulent vortices in the wake of a cylinder. *J. Fluid Mech.* 253, 643–661.